



# CHALMERS

## Chalmers Publication Library

### Demonstration of post-growth wavelength setting of VCSELs using high-contrast gratings

This document has been downloaded from Chalmers Publication Library (CPL). It is the author's version of a work that was accepted for publication in:

**Optics Express (ISSN: 1094-4087)**

#### Citation for the published paper:

Haglund, E. ; Gustavsson, J. ; Bengtsson, J. et al. (2016) "Demonstration of post-growth wavelength setting of VCSELs using high-contrast gratings". Optics Express, vol. 24(3), pp. 1999-2005.

<http://dx.doi.org/10.1364/oe.24.001999>

Downloaded from: <http://publications.lib.chalmers.se/publication/234227>

Notice: Changes introduced as a result of publishing processes such as copy-editing and formatting may not be reflected in this document. For a definitive version of this work, please refer to the published source. Please note that access to the published version might require a subscription.

Chalmers Publication Library (CPL) offers the possibility of retrieving research publications produced at Chalmers University of Technology. It covers all types of publications: articles, dissertations, licentiate theses, masters theses, conference papers, reports etc. Since 2006 it is the official tool for Chalmers official publication statistics. To ensure that Chalmers research results are disseminated as widely as possible, an Open Access Policy has been adopted. The CPL service is administrated and maintained by Chalmers Library.

# Demonstration of post-growth wavelength setting of VCSELs using high-contrast gratings

E. Haglund,<sup>1,\*</sup> J.S. Gustavsson,<sup>1</sup> J. Bengtsson,<sup>1</sup> Å. Haglund,<sup>1</sup> A. Larsson,<sup>1</sup> D. Fattal,<sup>2</sup> W. Sorin,<sup>3</sup> and M. Tan<sup>3</sup>

<sup>1</sup>Photonics Laboratory, Department of Microtechnology and Nanoscience, Chalmers University of Technology, SE-41296 Göteborg, Sweden

<sup>2</sup>LEIA Inc., 2440 Sand Hill Road, Menlo Park, CA 94025, USA

<sup>3</sup>HP Labs, 1501 Page Mill Road, Palo Alto, CA 94304-1123, USA

[erik.haglund@chalmers.se](mailto:erik.haglund@chalmers.se)

**Abstract:** We demonstrate, for the first time, post-growth wavelength setting of electrically-injected vertical-cavity surface-emitting lasers (VCSELs) by using high-contrast gratings (HCGs) with different grating parameters. By fabricating HCGs with different duty cycle and period, the HCG reflection phase can be varied, in effect giving different optical cavity lengths for HCG-VCSELs with different grating parameters. This enables fabrication of monolithic multi-wavelength HCG-VCSEL arrays for wavelength-division multiplexing (WDM). The GaAs HCG is suspended in air by removing a sacrificial layer of InGaP. Electrically-injected 980-nm HCG-VCSELs with sub-mA threshold currents indicate high reflectivity from the GaAs HCGs. Lasing over a wavelength span of 15 nm was achieved, enabling a 4-channel WDM array with 5 nm channel spacing. A large wavelength setting span was enabled by an air-coupled cavity design and the use of only the HCG as top mirror.

©2016 Optical Society of America

**OCIS codes:** (050.2770) Gratings; (050.6624) Subwavelength structures; (140.7260) Vertical cavity surface emitting lasers.

---

## References and links

1. N. Chitica, J. Carlsson, L.-G. Svensson, and M. Chacinski, "Vertical cavity surface emitting lasers enable high-density ultra-high bandwidth optical interconnects," Proc. SPIE **9381**, 938103 (2015).
2. P. Westbergh, J. S. Gustavsson, and A. Larsson, "VCSEL arrays for multicore fiber interconnects with an aggregate capacity of 240 Gbit/s," IEEE Photonics Technol. Lett. **27**(3), 296–299 (2015).
3. J. A. Tatum, D. Gazula, L. A. Graham, J. K. Guenter, R. H. Johnson, J. King, C. Kocot, G. D. Landry, I. Lyubomirsky, D. Vaidya, M. Yan, and F. Tang, "VCSEL-based interconnects for current and future data centers," J. Lightwave Technol. **33**(4), 727–732 (2015).
4. A. Larsson, "Advances in VCSELs for communication and sensing," IEEE J. Sel. Top. Quantum Electron. **17**(6), 1552–1567 (2011).
5. D. M. Kuchta, A. V. Rylyakov, F. Doany, C. L. Schow, J. E. Proesel, C. W. Baks, P. Westbergh, J. S. Gustavsson, and A. Larsson, "A 71 Gb/s NRZ modulated 850 nm VCSEL-based optical link," IEEE Photonics Technol. Lett. **27**(6), 577–580 (2015).
6. E. Haglund, P. Westbergh, J. S. Gustavsson, E. P. Haglund, A. Larsson, M. Geen, and A. Joel, "30 GHz bandwidth 850 nm VCSEL with sub-100 fJ/bit energy dissipation at 25–50 Gbit/s," Electron. Lett. **51**(14), 1096–1098 (2015).
7. C. J. Chang-Hasnain, M. W. Maeda, J. P. Harbison, L. T. Florez, and C. Lin, "Monolithic multiple wavelength surface emitting laser arrays," J. Lightwave Technol. **9**(12), 1665–1673 (1991).
8. M. Arai, T. Kondo, A. Onomura, A. Matsutani, T. Miyamoto, and F. Koyama, "Multiple-wavelength GaInAs-GaAs vertical cavity surface emitting laser array with extended wavelength span," IEEE J. Sel. Top. Quantum Electron. **9**(5), 1367–1373 (2003).
9. J. Geske, Y. L. Okuno, D. Leonard, and J. Bowers, "Long wavelength two-dimensional WDM vertical cavity surface emitting laser arrays fabricated by nonplanar wafer bonding," IEEE Photonics Technol. Lett. **15**(2), 179–181 (2003).
10. A. Fiore, Y. Akulova, J. Ko, E. Hegblom, and L. Coldren, "Postgrowth tuning of semiconductor vertical cavities for multiple-wavelength laser arrays," IEEE J. Quantum Electron. **35**(4), 616–623 (1999).

11. T. Wipiejewski, M. Peters, E. Hegblom, and L. Coldren, "Vertical-cavity surface-emitting laser diodes with post-growth wavelength adjustment," *IEEE Photonics Technol. Lett.* **7**(7), 727–729 (1995).
12. P. B. Dayal, T. Sakaguchi, A. Matsutani, and F. Koyama, "Multiple-wavelength vertical-cavity surface-emitting lasers by grading a spacer layer for short-reach wavelength division multiplexing applications," *Appl. Phys. Express* **2**(9), 092501 (2009).
13. J. H. E. Kim, L. Chrostowski, E. Bisaillon, and D. V. Plant, "DBR, Sub-wavelength grating, and Photonic crystal slab Fabry-Perot cavity design using phase analysis by FDTD," *Opt. Express* **15**(16), 10330–10339 (2007).
14. V. Karagodsky, B. Pesala, C. Chase, W. Hofmann, F. Koyama, and C. J. Chang-Hasnain, "Monolithically integrated multi-wavelength VCSEL arrays using high-contrast gratings," *Opt. Express* **18**(2), 694–699 (2010).
15. C. Sciancalepore, B. Bakir, S. Menezo, X. Letartre, D. Bordel, and P. Viktorovitch, "III-V-on-Si photonic crystal vertical-cavity surface-emitting laser arrays for wavelength division multiplexing," *IEEE Photonics Technol. Lett.* **25**(12), 1111–1113 (2013).
16. Y. Rao, C. Chase, and C. J. Chang-Hasnain, "Multiwavelength HCG-VCSEL array," in *Proceedings of 22nd International Semiconductor Laser Workshop* (IEEE, 2010), pp. 11–12.
17. F. Sugihwo, M. Larson, and J. S. Harris, "Micromachined widely tunable vertical cavity laser diodes," *J. Microelectromech. Syst.* **7**(1), 48–55 (1998).
18. W. Hofmann, C. Chase, M. Müller, Y. Rao, C. Grasse, G. Böhm, M.-C. Amann, and C. J. Chang-Hasnain, "Long-wavelength high-contrast grating vertical-cavity surface-emitting laser," *IEEE Photonics J.* **2**(3), 415–422 (2010).
19. T. Ansbaek, I.-S. Chung, E. Semenova, and K. Yvind, "1060-nm tunable monolithic high index contrast subwavelength grating VCSEL," *IEEE Photonics Technol. Lett.* **25**(4), 365–367 (2013).
20. C. Chang-Hasnain, Y. Zhou, M. Huang, and C. Chase, "High-contrast grating VCSELs," *IEEE J. Sel. Top. Quantum Electron.* **15**(3), 869–878 (2009).
21. S. Inoue, J. Kashino, A. Matsutani, H. Ohtsuki, T. Miyashita, and F. Koyama, "Highly angular dependent high-contrast grating mirror and its application for transverse-mode control of VCSELs," *Jpn. J. Appl. Phys.* **53**(9), 090306 (2014).
22. D. B. Young, J. W. Scott, F. H. Peters, M. G. Peters, M. L. Majewski, B. J. Thibeault, S. W. Corzine, and L. A. Coldren, "Enhanced performance of offset-gain high-barrier vertical-cavity surface-emitting lasers," *IEEE J. Quantum Electron.* **29**(6), 2013–2022 (1993).
23. M. J. Cich, J. A. Johnson, G. M. Peake, and O. B. Spahn, "Crystallographic dependence of the lateral undercut wet etching rate of InGaP in HCl," *Appl. Phys. Lett.* **82**(4), 651–653 (2003).

## 1. Introduction

To meet requirements of higher interconnect capacity in datacenters and high performance computing systems, optical interconnects (OIs) are evolving towards higher data rates on several lanes using parallel optical fibers [1]. Even higher aggregate capacities and improved bandwidth densities are enabled by multicore fibers [2]. Yet another technique for increasing capacity and bandwidth density is wavelength-division multiplexing (WDM) [3]. The use of multiple wavelengths on multiple fibers with multiple cores, together with higher lane rates enabled by higher speed optoelectronics and electronics, electronic compensation techniques, and multilevel modulation, may eventually provide >100 Tbit/s interconnect cable capacity.

The vertical-cavity surface-emitting laser (VCSEL) is a light source most suitable for OIs [4]. VCSEL-based OIs have reached >70 Gbit/s lane rates [5], low power dissipation at high bit rates [6], and VCSEL arrays together with multicore fibers have enabled 240 Gbit/s aggregate capacity on a single fiber [2]. The use of VCSELs for WDM-OIs would benefit from the development of monolithic multi-wavelength VCSEL arrays. However, monolithic arrays are intrinsically difficult to realize due to the fact that the resonance wavelength of the conventional all-semiconductor VCSEL cavity, defined by the reflection phase of the top and bottom distributed Bragg reflectors (DBRs) and the thickness of the active region separating the DBRs, is set during epitaxial growth. Therefore, modified growth techniques such as non-uniform growth by molecular beam epitaxy [7], growth on nonplanar substrates by metal-organic chemical vapor deposition (MOCVD) [8], as well as assembly techniques such as nonplanar wafer bonding [9] have been investigated to achieve a resonance wavelength variation across the wafer. However, these techniques are not suitable for small-footprint dense VCSEL arrays with arbitrary layout. Various techniques for post-growth intra-cavity phase tuning have also been investigated, including lateral-vertical oxidation [10] and deposition or thinning of an intra-cavity phase tuning layer prior to the deposition of a dielectric top DBR [11,12]. Another possibility is to replace the top DBR with a

subwavelength high-contrast grating (HCG) and make use of the dependence of the HCG reflection phase on the grating parameters. Multi-wavelength emission can then be achieved by varying the HCG period and/or duty cycle over the VCSEL array. A major advantage of using HCGs is that the resonance wavelength can be set in a single lithography and etch step, relying on the high precision of electron-beam lithography, while the following etch steps do not require very precise control of etch time and etch depth. This technique has been proposed and analyzed theoretically [13,14], and experimentally demonstrated by optical pumping experiments [15]. However, electrically-injected multi-wavelength HCG-VCSEL arrays with wavelengths set by the grating parameters have so far not been demonstrated, since HCGs with exceptionally high reflectivity are needed. A multiwavelength HCG-VCSEL array has previously been demonstrated by using different air-gap thickness underneath suspended HCGs [16]. All HCGs had the same period and duty cycle, and therefore the wavelength-setting was not accomplished using a variation of the HCG parameters.

Here we report on the first experimental demonstration of post-growth wavelength setting of electrically-injected HCG-VCSELs using the grating parameters. The HCG-VCSELs are GaAs-based and employ a suspended GaAs HCG as top mirror. A wavelength span of 15 nm, centered at 985 nm, is covered by varying the HCG duty cycle from 54 to 69%, in good agreement with calculations.

## 2. WDM HCG-VCSEL design

The phase of the reflection from the suspended HCG is strongly dependent on the grating period, duty cycle, and thickness. Rigorous coupled-wave analysis (RCWA) simulations, seen in Fig. 1, show that the GaAs HCG can achieve high reflectivity ( $>99.8\%$ ) for HCGs with a range of different period and duty cycle combinations. The HCGs are designed for transverse magnetic (TM) polarization. By changing duty cycle and/or period, a reflection phase span of  $>60^\circ$  is achievable (Fig. 1). Therefore, HCG-VCSEL resonators with different HCG parameters will have different phase shifts from the HCG reflection, leading to different resonance wavelengths, as seen in Fig. 2. A change in the HCG reflection phase will have the same effect as a phase shift obtained by changing the thickness of the air-gap below the HCG, as commonly done in tunable MEMS-VCSELs [17]. To obtain the largest possible wavelength span for the array, the resonance wavelength of the laser cavity must be highly sensitive to the HCG reflection phase. With few exceptions [18,19], previously demonstrated HCG-VCSELs

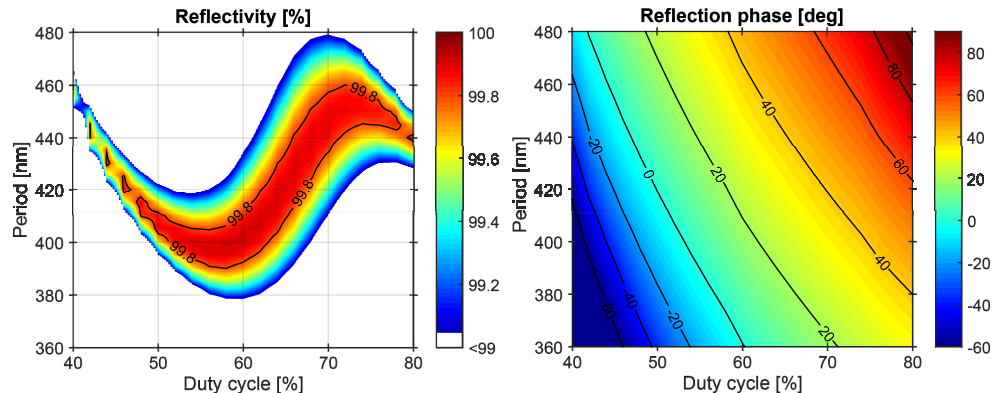


Fig. 1. HCG reflectivity (left) and reflection phase (right) at 980 nm for different grating parameters, simulated using RCWA for a grating thickness of 270 nm.

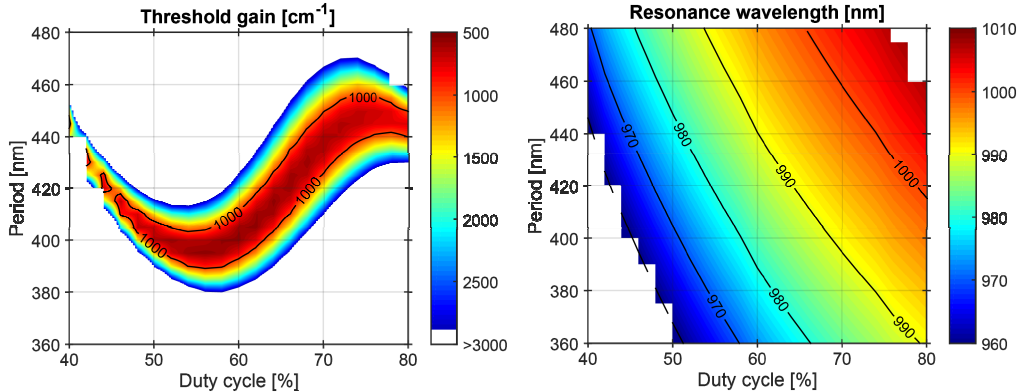


Fig. 2. Calculated material gain at threshold (left) and resonance wavelength (right) for HCG-VCSELs with different HCG parameters.

typically have hybrid top mirrors where the HCG reflectivity is boosted by 2-4 DBR pairs [20,21]. This makes the resonance wavelength relatively insensitive to the HCG reflection phase and a wavelength range of only  $\sim 2$  nm is obtained by changing the HCG parameters [20]. Even if the DBR pairs are removed, the obtainable wavelength span is still strongly dependent on the configuration of the cavity, in particular the position of the intra-cavity semiconductor-air interface with respect to the standing optical wave. It is well known from tunable MEMS-VCSEL design that the best tuning efficiency is obtained if the semiconductor-air interface is placed at a node of the standing wave [17]. This cavity configuration is known as an air-coupled cavity. In our air-coupled cavity design (Fig. 3), the air gap below the HCG is  $\lambda/2$  thick and the current-spreading layer above the active region is  $3\lambda/4$  thick. The resonance wavelength and threshold material gain for HCG-VCSELs with different HCG parameters were calculated using a 1-dimensional transfer-matrix model, using the HCG properties from the RCWA simulations. As seen in Fig. 2, a wide wavelength span of 40 nm can be obtained with threshold material gain  $<1000$   $\text{cm}^{-1}$ , using HCGs with duty cycles of 45-75% and periods of 400-450 nm. On average, the resonance wavelength changes about 1 nm per percentage change in duty cycle and 0.2 nm per nm change in period.

In the air-coupled cavity configuration the air gap acts as the optical cavity, strongly confining the optical field to the air gap, while the current-spreading layer and active region can be viewed as part of the bottom DBR (see Fig. 3(b)). This results in a small longitudinal optical confinement factor  $\Gamma$  of around 0.6%. As an example, for HCG reflectivities of 99.8%, the numerically calculated material gain at threshold is therefore as high as 1000  $\text{cm}^{-1}$ . For an equivalent structure with the semiconductor-air interface at an antinode of the standing wave, the same HCG reflectivity yields a much lower threshold gain of 300  $\text{cm}^{-1}$ . However, the achievable wavelength span is then 5-10 times smaller.

A schematic figure of the HCG-VCSEL can be seen in Fig. 3(a). The active region features three 6 nm thick strained  $\text{In}_{0.18}\text{Ga}_{0.82}\text{As}$  quantum wells (QWs) with  $\text{GaAs}_{0.92}\text{P}_{0.08}$  strain compensating barriers. The QW photoluminescence (PL) peak was 969 nm, measured at low excitation on a calibration sample. We therefore expect the gain peak at around 985 nm at the high excitation needed for lasing [22]. The bottom  $n$ -DBR has 37 pairs of  $\text{Al}_{0.90}\text{Ga}_{0.10}\text{As}/\text{GaAs}$ . Holes are injected through the  $3\lambda/4$ -thick  $p$ -GaAs current spreading layer which is modulation doped for low resistance and low free-carrier absorption. Transverse current and optical confinement is provided by an oxide aperture on each side of the active region. The 270 nm thick GaAs HCG layer is grown on top of the lattice-matched  $\text{In}_{0.49}\text{Ga}_{0.51}\text{P}$  sacrificial layer. InGaP was used instead of InAlP [19] or AlGaAs to avoid problems with oxidation of the remaining sacrificial layer. After selective removal, the

sacrificial layer forms a  $\lambda/2$ -thick air gap. A free-carrier absorption in the HCG of  $35 \text{ cm}^{-1}$  due to  $p$ -doping at  $5 \cdot 10^{18} \text{ cm}^{-3}$  was included in the RCWA simulations.

### 3. HCG-VCSEL fabrication

The epitaxial structure was grown by MOCVD on an  $n$ -doped (100) GaAs wafer, with a  $10^\circ$  off-cut towards  $\langle 111 \rangle$  in order to suppress ordering of the InGaP layer. Multi-wavelength HCG-VCSEL arrays with  $350 \mu\text{m}$  device pitch were subsequently fabricated using standard VCSEL processing techniques. The device pitch can be reduced considerably, and will ultimately be limited by the mesa size. First, Ti/Pt/Au top  $p$ -contacts and Ni/Ge/Au backside  $n$ -contacts were deposited. Mesas with a diameter of  $40\text{-}50 \mu\text{m}$  were then etched in a three-step etch process. Initially, the top GaAs layer was removed using  $\text{SiCl}_4/\text{Ar}$ -based inductively coupled plasma (ICP) reactive ion etching (RIE). Since the InGaP of the sacrificial layer etches poorly in this chemistry, it was removed by wet etching using concentrated HCl in a second step. Finally, the ICP-RIE dry etch was used to etch partly into the  $n$ -DBR to expose the two  $30 \text{ nm}$  thick  $\text{Al}_{0.98}\text{Ga}_{0.02}\text{As}$  layers used for the formation of current apertures in the following selective wet oxidation step. Benzocyclobutene (BCB) was used to planarize the structure and  $p$ -bondpads were deposited. The HCGs were defined by electron-beam lithography in  $400 \text{ nm}$  thick ZEP520A resist. After dry etching into the sacrificial layer using a highly anisotropic  $\text{SiCl}_4$  RIE

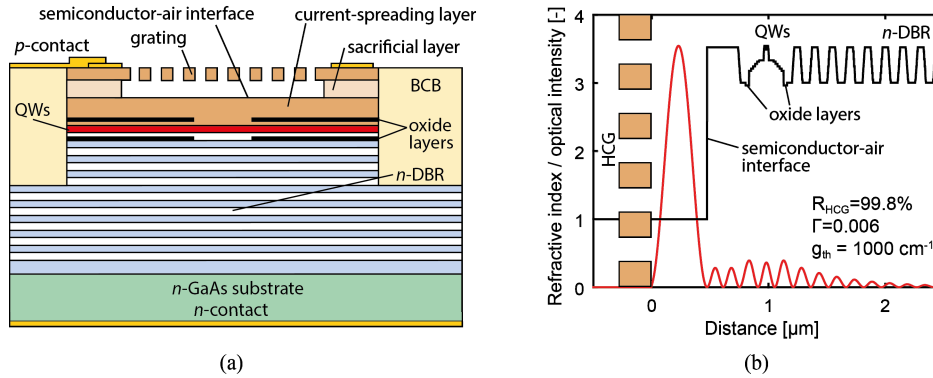


Fig. 3. (a) Schematic figure of the HCG-VCSEL. (b) Refractive index profile and calculated optical field intensity for a HCG-VCSEL with 99.8% HCG reflectivity. This is an air-coupled design, thus the optical field has a node at the semiconductor-air interface.

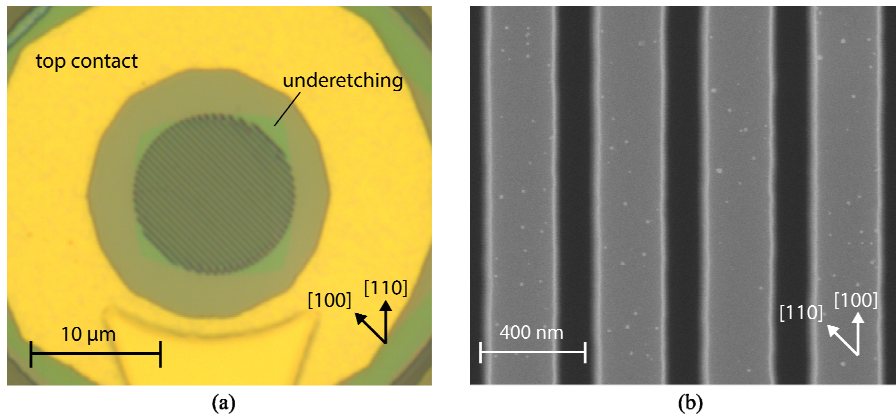


Fig. 4. (a) Microscope image of a fabricated HCG-VCSEL. The underetching in  $\langle 100 \rangle$  is seen in the corners of the HCG. (b) Close-up SEM image of a HCG with a period of  $416 \text{ nm}$  and duty-cycle of 64%. Note that the images have different crystal orientations.

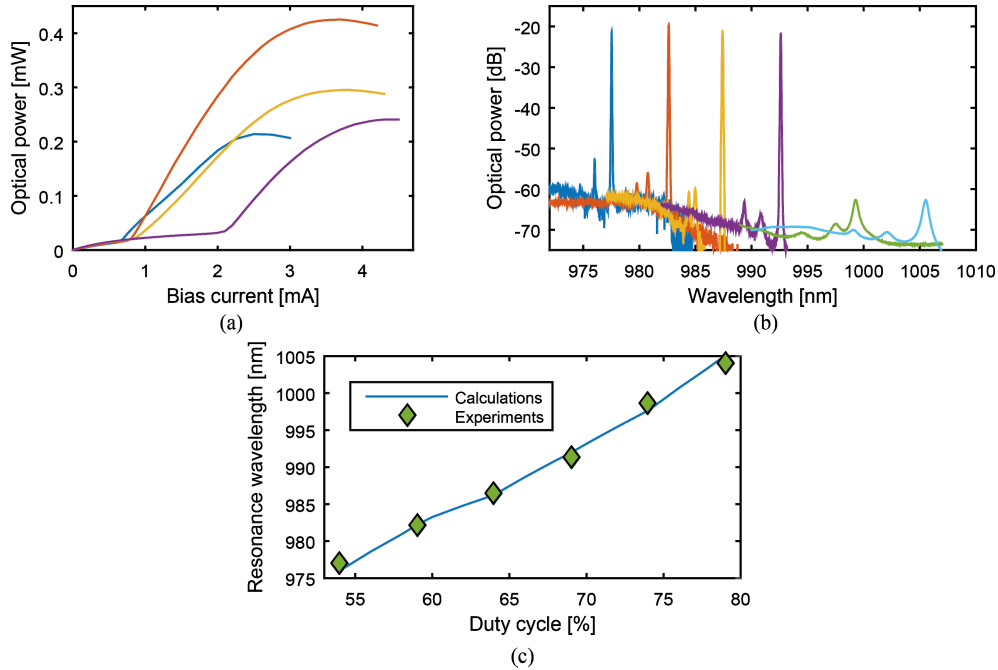


Fig. 5. Room-temperature characteristics for VCSELs with different HCG period and duty cycle. (a) Output power vs. current. (b) Optical spectra measured at 2 mA (3 mA for the longest-wavelength lasing, and the non-lasing devices). (c) Comparison of resonance wavelengths measured at 1 mA with numerical calculations. HCG period/duty cycle, from short to long wavelength, is: 405 nm/54%, 405 nm/59%, 400 nm/64%, 410 nm/69%, 425 nm/74%, and 450 nm/79%.

dry etch, the sacrificial InGaP layer was selectively removed using concentrated HCl. As the HCl does not etch GaAs, except for the  $\sim 1$  nm thick native oxide, InGaP may be etched with a selectivity to GaAs approaching infinity. However, the etch rate depends on the crystal orientation and the InGaP will underetch in  $\langle 100 \rangle$ , but not  $\langle 110 \rangle$  [23]. The grating lines were therefore oriented along  $\langle 100 \rangle$ , at a  $45^\circ$  angle to the  $\{110\}$  cleavage planes. Each resist removal was performed using a combination of standard solvents, O<sub>2</sub>-ashing, and ozone cleaning. Especially ozone cleaning was found to be of vital importance for successful removal of the InGaP sacrificial layer. After selective removal, drying was accomplished using critical point drying to avoid stiction. Microscope and close-up SEM images of an HCG-VCSEL with a suspended GaAs HCG are shown in Fig. 4. No buckled grating beams were observed for any fabricated gratings, with diameters up to 22  $\mu\text{m}$ , indicating low stress in the GaAs HCG layer.

#### 4. Measurements

HCG-VCSELs with oxide aperture diameters of 5  $\mu\text{m}$  and different HCG period/duty cycle combinations were characterized by output power and spectral measurements. As seen in Fig. 5(a), lasing was observed for a range of different HCG parameters with sub-mA thresholds for several VCSELs. The low threshold currents, despite the air-coupled cavity configuration, indicate very high HCG reflectivity, comparable to, or even better than, the top DBRs used in our conventional VCSELs. The low slope efficiencies and early thermal roll-over may be caused by a combination of effects such as high optical loss due to free-carrier absorption in the doped HCG and current-spreading layer, too high HCG reflectivity leading to low out-coupling of light from the cavity, or non-uniform current injection through the thin current-spreading layer. Owing to the angular-dependent reflectivity of HCGs [21], highly single-

mode emission with a side-mode suppression ratio of 30-40 dB was observed (Fig. 5(b)). With small variations of the HCG period, and duty cycles from 54 to 69%, lasing over a span of 15 nm was realized, enabling a multi-wavelength VCSEL array with a channel spacing of 5 nm centered at 985 nm. A red-shift with increasing bias of about 0.22 nm/mW dissipated power was observed, which is the same as in our conventional VCSELs featuring two epitaxial DBRs [6]. Even longer-wavelength resonances were measured for larger duty cycles, but are too far away from the QW gain peak to reach lasing. The observed resonance wavelengths agree well with our calculations, see Fig. 5(c).

## 5. Summary and conclusions

For the first time, the dependence of the HCG reflection phase on the grating parameters was used to demonstrate post-growth wavelength setting of electrically-injected HCG-VCSELs. An air-coupled cavity configuration was used to increase the sensitivity of the resonance wavelength to a variation of the grating parameters, thus enabling a large wavelength span. In spite of the low optical confinement factor for this cavity configuration, VCSELs with low threshold currents were demonstrated, indicating very high HCG reflectivities. Lasing was observed over a wavelength span of 15 nm, in excellent agreement with numerical calculations. This has enabled a 4-channel monolithic multi-wavelength VCSEL array with a channel spacing of 5 nm. In addition, this is the first report on suspended GaAs HCGs using an InGaP sacrificial layer, which may be selectively etched with high selectivity.

## Acknowledgments

This project was financially supported by Hewlett Packard Labs, the Swedish Foundation for Strategic Research, and the Swedish Research Council. The authors would also like to acknowledge valuable technical discussions with Dr. Marco Fiorentino and Dr. Sagi Mathai at Hewlett Packard. The epitaxial material was provided by IQE Europe.